2009 American Control Conference
Hyatt Regency Riverfront, St. Louis, MO, USA
June 10-12, 2009



# LPV control of an active vibration isolation system

W.H.T.M. Aangenent, C.H.A. Criens, M.J.G. van de Molengraft, M.F. Heertjes, and M. Steinbuch
*Department of Mechanical Engineering, Eindhoven University of Technology*

***Abstract*— Non-stationary disturbances in motion systems generally limit the closed-loop performance. If these disturbance can be measured, this measurement can be used to enable a linear parameter varying (LPV) controller to adapt itself to the current operating condition, resulting in a closed-loop system with an overall increased performance. In this paper, this idea is applied to an active vibration isolation system.**

***Index Terms*— LPV, vibration isolation, frequency estimator**

## I. INTRODUCTION

In high-precision motion systems, vibrations of unknown frequency and amplitude can severely limit performance. These vibrations can for instance be induced by floor vibrations that are transferred to the system or by forces that directly act on the system such as (conditional) flows. Examples of processes where this occurs include high-resolution measurement equipment such as scanning electron microscopes [1] used for sub-micron imaging, and photolithographic wafer steppers and scanners [2] used for fabrication of integrated circuits. For these systems, the typical amplitudes of the induced vibrations are of the same magnitude as the dimensions of the measured or manufactured objects, and therefore these vibrations limit performance. To provide such systems with a vibration free platform, vibration isolation systems are used, where disturbance isolation is achieved passively, actively, or both [3]. Figure 1 shows a schematic representation of such a vibration isolation system. Herein, $k$, $b$ are the isolator stiffness and damping, respectively, $d$ represents the floor vibrations and $f_d$ denotes the disturbance forces that act directly on the payload. The payload displacement in vertical direction is denoted by $y$, and $f_a$ is the force generated by an actuator. The goal of a vibration isolation system is to minimize the effect of the environmental disturbances $d$ and $f_d$ on the vertical velocity $v = \dot{y}$ of the payload. The passive part of the vibration isolation system consists of a heavy payload supported by elastic springs and damping units, resulting in a mechanical low-pass system with typical resonance frequencies between 2 and 5 Hertz. Since the passive system is generally weakly damped, disturbance amplification at the natural frequency is often observed. Increasing the structural damping of the system may offer a solution, however, a major disadvantage of passive damping is that the disturbance rejection properties deteriorate [4]. This is illustrated in Figure 2, where a typical frequency response of the transfer from $f_d$ to $y$ is depicted. Moreover, the passive type is, in principle, unable to attenuate disturbances $f_d$ that directly act on the payload such as an exiting force generated in a mounted operating machine, an airflow from the air conditioning,

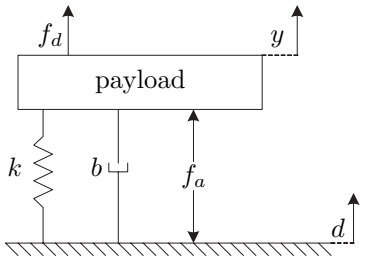


Fig. 1. Schematic representation of a vibration isolation system.

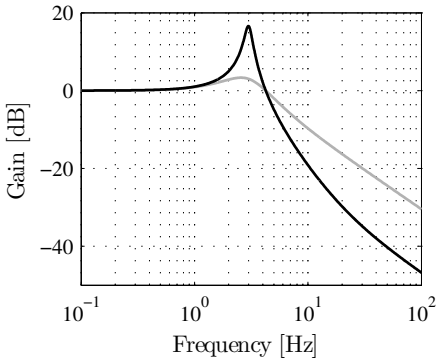


Fig. 2. Mechanical low-pass characteristic of a passive isolation system with low (black) and high (grey) structural damping.

and acoustic excitations. By applying active damping near the natural frequency of the passive system, i.e., by active vibration isolation, a significant benefit in vibration isolation can be obtained.

In the active vibration isolation system (AVIS) we consider, active vibration isolation is achieved by controlled actuation of the payload, based on feedback of its payload velocity. The payload velocity is directly measured through geophones while the actuation is performed by means of Lorentz actuators. A picture of the AVIS is shown in Figure 3(a). In this paper, the payload of the AVIS is used as an experimental benchmark representing a metrology frame that needs to be isolated from environmental disturbances. This means that the amplitude of the vertical velocity $v$ should be controlled to be as low as possible. A machine is mounted to this metrology frame that performs periodic tasks, which result in non-stationary environmental disturbances $f_d$ with frequency content between $4$ and $10$ Hz, depending on the specific task that is performed. This machine is represented by a rotational imbalance, depicted in Figure 3. The induced disturbances $f_d$ are not known beforehand and cannot be

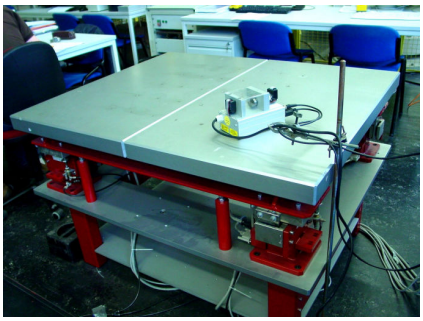

(a)

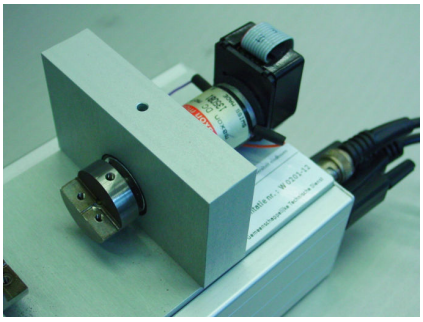

(b)

Fig. 3. (a) The active vibration isolator platform including the mounted rotating imbalance, (b) a close-up of the rotating imbalance.

measured directly. As a consequence, direct disturbance compensation via feedforward cannot be applied. Although other disturbance sources are present as well, the periodic disturbance generated by the mounted machine is expected to dominate the measured output. All that is known about the induced disturbance is that it consists of a single, time-varying frequency in the range between $4$ and $10$ Hz. The objective is to improve the isolation performance beyond the level of a commonly used linear time invariant (LTI) controller. Although such an LTI controller reduces the effect of disturbances in the frequency range $4$ to $10$ Hz, the achieved isolation performance is considered not to be adequate. To improve the isolation performance, the LTI controller will be adjusted in order to provide additional disturbance reduction.

A classical solution to reduce disturbances at specific frequencies is the use of an inverted notch filter in the controller to increase the gain at that frequency. Such a notch filter results in a decreased sensitivity for disturbances in a small frequency range around the center frequency of the notch. Unfortunately, a classical notch filter cannot be applied to the posed problem for two reasons. Firstly, the frequency of the expected periodic disturbance varies in an interval between $4$ and $10$ Hz, while a fixed notch is only effective around a single frequency. Secondly, even if the disturbance signal would be stationary instead of time-varying (for instance when the mounted machine is operating in a stationary condition), the actual disturbance frequency, and hence the target center frequency of the notch, is not known beforehand.

In this paper, we propose a solution to improve the isolation performance that circumvents these two problems. The problem of the unknown frequency will be tackled by devising an algorithm that identifies the dominating disturbance frequency from available measured data from the AVIS. The problem of frequency variation can be solved by extending controller (2) with a notch of which the center frequency can be varied. This way, a linear parameter varying (LPV) controller is obtained that can adapt the center frequency of the notch to the identified disturbance frequency, resulting in an improved isolation performance at that frequency.

The paper is organized as follows. In Section II the spectral analysis method to identify the dominating disturbance frequency is discussed. The design of the LPV controller is done in Section III, while the closed-loop stability is assessed in Section IV. The interconnection of the signal analyzer and the controller is treated in Section V while the proposed approach is simulated in Section VI. Experimental validation is done in Section VII. Finally, we conclude in Section VIII.

## II. Spectral analysis

The posed problem requires a frequency identifier that is able to determine the actual frequency of the disturbance from the measured signals of the AVIS. Since the proposed LPV controller is required to adapt itself to the disturbance that acts on the system, the disturbance frequency at the current time instant should be available. This information can be obtained through time-frequency spectral analysis. Since in practical applications low frequency components often last a long period of time, while high frequency components often appear as short bursts, a so-called multiresolution spectrum is desirable. A multiresolution spectrum combines a high frequency resolution (with a corresponding low time resolution) for low frequencies with a high time resolution (and hence a low frequency resolution) for high frequencies. The wavelet transform [5] was developed to obtain such a multiresolution analysis. Therefore, we use wavelet analysis to obtain a spectrum analyzer which provides the dominating disturbance frequency at the current time. The wavelet that is used is a truncated Morlet wavelet [5] and the real-time implementation of the transformation is inspired by [6].

## III. Controller design

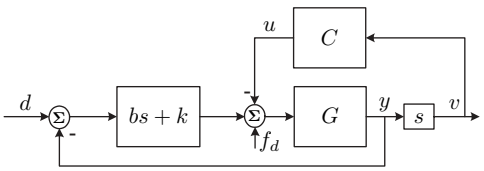


Fig. 4. schematic of the controlled isolation system.

The schematic of one of the controlled vibration isolators is depicted in Figure 4, where $u = f_a$ is the controller output, $v = \dot{y}$ is the payload velocity in vertical direction, $G$ denotes the transfer function of an isolator module, and $C$ is the

controller. A fourth-order model of an isolator of the AVIS is given by the transfer function [7]

$$G(s) = \frac{m_2 s^2 + b_{12} s + k_{12}}{m_1 m_2 s^4 + (m_1 + m_2)(b_{12} s^3 + k_{12})}, \quad (1)$$

with $m_1 = 950$ kg, $m_2 = 50$ kg, $b_{12} = 3 \cdot 10^2$ Nsm$^{-1}$, and $k_{12} = 1.75 \cdot 10^6$ Nm$^{-1}$. The isolator's passive stiffness and damping are $k = 4.25 \cdot 10^5$ Nm$^{-1}$ and $b = 2 \cdot 10^3$ Nsm$^{-1}$, respectively. To reduce the effect of disturbances near the resonance frequency, controller $C$ is designed as the complex valued damper [7]

$$C(s) = k_d \left( \frac{s}{s + \omega_{hp}} \right)^2 \left( \frac{\omega_{lp}}{s + \omega_{lp}} \right)^2, \quad (2)$$

which consists of a gain $k_d$, combined with a low-pass filter with cut-off frequency $\omega_{lp}$, and a high-pass filter with cut-off frequency $\omega_{hp}$. The choices for $\omega_{hp}$ and $\omega_{lp}$ are related to the limitations of the sensors and actuators, respectively. Since the geophones produce unreliable output below 0.1 Hz, and since actuator limitations occur beyond 100 Hz, the cut-off frequencies are chosen as $\omega_{hp} = 0.2\pi$ rad/s and $\omega_{lp} = 200\pi$ rad/s, and the gain is $k_d = 3 \cdot 10^4$ Nsm$^{-1}$. This controller is designed to preserve the desirable properties at high frequencies of the passive isolator, while it significantly reduces the effect of disturbances around the resonance frequency. In Figure 5 the Bode diagram of the uncontrolled plant (i.e., of the passive vibration isolation system)

$$P_p(s) = \frac{v(s)}{f_d(s)} = \frac{sG(s)}{1 + (bs + k)G(s)}, \quad (3)$$

is compared with that of the the controlled plant (i.e., of the active vibration isolation system)

$$P_a(s) = \frac{v(s)}{f_d(s)} = \frac{sG(s)}{1 + (bs + k)G(s) + sC(s)G(s)}. \quad (4)$$

The maximum amplitude occurs around the resonance frequency, which implies that the plant still is most sensitive to disturbances in this frequency region. However, the sensitivity in this region is reduced by about a factor 17. The price paid is a slightly increased amplitude between 10 and 20 Hz. The frequency of the dominating disturbance that acts on the system can be identified by using a wavelet-based algorithm as discussed in the previous section. This information can be used to adapt controller (2) in order to improve the isolation performance at that frequency. Such a controller can be designed via the LPV synthesis framework [8] using frequency and parameter dependent weightings expressing the desired performance. For this specific application however, it is expected that the desired performance can be achieved by extending controller (2) with an LPV notch filter, the center frequency of which is adapted to the identified disturbance frequency. Therefore, in this section we will design the controller by hand and analyze the closed-loop stability afterwards.

An LTI notch filter is described by the transfer function

$$H_n(s) = \frac{s^2 + 2\beta_1(2\pi f_n)s + (2\pi f_n)^2}{s^2 + 2\beta_2(2\pi f_n)s + (2\pi f_n)^2}, \quad (5)$$

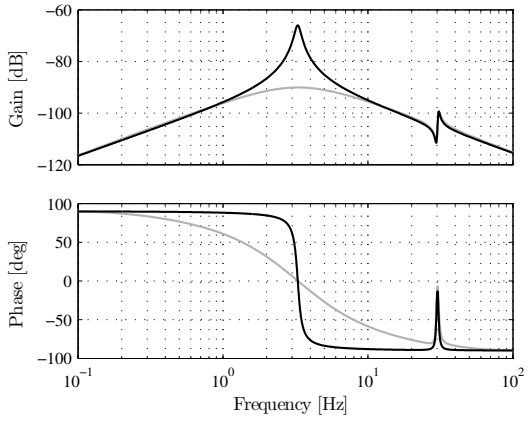


Fig. 5. The Bode diagram of the transfer function from the environmental disturbance $f_d$ to the measured output $v$ of the passive isolation system (black) and of the active isolation system (grey).

where $f_n$ is the center frequency in Hz, and $\beta_1$ and $\beta_2$ are parameters that can be used to alter the reduction factor and the width of the notch. Although ideally all three parameters $f_n$, $\beta_1$, and $\beta_2$ should be adapted depending on the disturbance characteristic, in this paper we only consider the adaptation of the center frequency $f_n$. Several factors play a role in the determination of the constant reduction factor and width of the notch filter. If only steady-state disturbance rejection around the center frequency $f_n$ is considered, a wide notch with a large reduction factor is desirable. Indeed, a wide notch will not only reduce disturbances at $f_n$, but has also good disturbance rejection properties for frequencies near $f_n$, while a larger reduction factor results in a higher reduction. Unfortunately, there are also downsides to using such a notch filter. Widening the filter reduces the disturbances in a larger area around the center frequency, but at the same time results in amplification of disturbances in another, larger, frequency region. This is illustrated in Figure 6(a), where the frequency response of the original actively controlled plant (4) is compared to that of the same controlled plant including a notch filter of different widths. The same holds if the reduction factor of the notch is increased. Another issue related to the width and reduction factor of a notch is its transient response time. A fast transient response of the notch filter is desirable since it allows a fast adaptation of the controller to the current disturbance frequency. A wide notch filter has a shorter transient response time than a narrow one, just as a filter with a smaller reduction factor has a shorter transient response time than one with a higher reduction factor. The effect on the transient response caused by widening the notch filter is illustrated in Figure 6(b), where the response of the controlled plant to a sinusoidal disturbance of 10 Hz is depicted with the same notch filters of different width.

The transient response time of the notch filter depends on the center frequency similarly as the frequency identification time of the real-time frequency analyzer. Therefore, in a

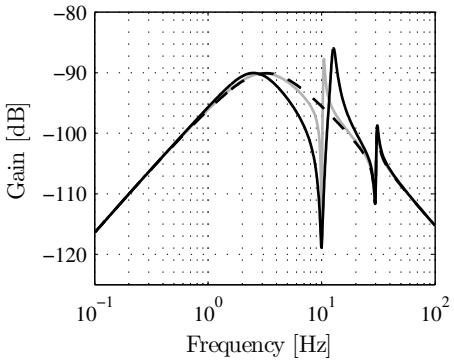


(a)

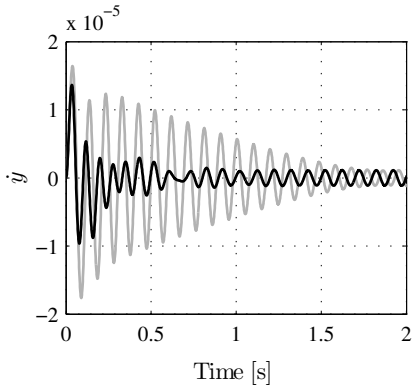


(b)

Fig. 6. Bode diagram of the original controlled plant (4) (dashed) and two notches of different widths (solid black and grey). (a) Effect of widening the notch on the frequency response, (b) effect of widening the notch on the transient response time.

proper overall controller design, the transient response time of the notch filter for a certain frequency, and the time it takes to identify that frequency should be matched. We will use a notch that reduces the amplitude of the identified sinusoidal disturbance to approximately half of the final reduction in 3 periods. Furthermore, we choose a reduction factor of 30. The above discussion results in $\beta_1 = 0.6$ and $\beta_2 = 0.02$.

## IV. State-space realization and stability

To arrive at a closed-loop state-space system from disturbance input $f_d$ to measured output $v$, we start by representing the uncontrolled AVIS (the passive vibration isolation system) (3) in state-space form as

$$\begin{aligned} \dot{x} &= Ax + Bf_d \\ v &= Cx, \end{aligned} \tag{6}$$

where $x \in \mathbb{R}^4$ is the state vector, and $A, B, C$ are matrices of appropriate dimensions. The state-space description of the original controller (2) is given by

$$\begin{aligned} \dot{x_o^c} &= A_o^c x_o^c + B_o^c v \\ u &= C_o^c x_o^c, \end{aligned} \tag{7}$$

where $x_o^c \in \mathbb{R}^4$ is the original controller state vector, and $A_o^c, B_o^c, C_o^c$ are matrices of appropriate dimensions. This controller will be augmented with a notch filter that adapts itself to the dominating disturbance. The LTI notch filter (5) can be changed to an LPV notch by using the center frequency as the scheduling variable, i.e., $\delta := 2\pi f_n$. This LPV notch can be represented by various state-space realizations. It is well-known that the complexity and conservatism of the stability and performance analysis of LPV systems depends on the type of parameter dependence of that system [8]. For instance, systems that are affinely parameterized allow for a quadratic stability analysis without a relaxation gap, and therefore we aim at an affinely parameterized closed-loop system. Since the state-space description of the controlled AVIS is affine in the controller state-space matrices, an affinely parameterized state-space description of the controller results in an affinely parameterized state-space description of the controlled AVIS.

The LPV notch will be described by the modal canonical state-space representation

$$\left[\begin{array}{c|c} \dot{x}_\delta^c & \\ \hline u & \end{array}\right] = \left[\begin{array}{c|c} A_\delta^c(\delta) & B_\delta^c(\delta) \\ \hline C_\delta^c(\delta) & D_\delta^c(\delta) \end{array}\right] \left[\begin{array}{c|c} x_\delta^c & \\ \hline v & \end{array}\right], \tag{8}$$

where $x_\delta^c \in \mathbb{R}^2$ is the notch state vector and where

$$\left[\begin{array}{c|c} A_\delta^c(\delta) & B_\delta^c(\delta) \\ \hline C_\delta^c(\delta) & D_\delta^c(\delta) \end{array}\right] = \left[\begin{array}{cc|c} -\delta\beta_2 & -\delta\sqrt{-\beta_2^2+1} & \delta \\ \delta\sqrt{-\beta_2^2+1} & -\delta\beta_2 & \delta \\ \hline \frac{(\beta_1-\beta_2)\left(\beta_2^2-\beta_2\sqrt{-\beta_2^2+1}-1\right)}{\beta_2^2-1} & \frac{(\beta_1-\beta_2)\left(\beta_2^2+\beta_2\sqrt{-\beta_2^2+1}-1\right)}{\beta_2^2-1} & 1 \end{array}\right], \tag{9}$$

which is indeed affine in $\delta$. The series connection of (8) and the original controller (7) results in the affine parameter dependent controller

$$\left[\begin{array}{c|c} \dot{x}_c & \\ \hline u & \end{array}\right] = \left[\begin{array}{c|c} A_c(\delta) & B_c(\delta) \\ \hline C_c(\delta) & D_c(\delta) \end{array}\right] \left[\begin{array}{c|c} x_c & \\ \hline v & \end{array}\right], \tag{10}$$

where $x_c^T = [x_\delta^{cT}\ x_o^{cT}]^T$ and

$$\left[\begin{array}{c|c} A_c(\delta) & B_c(\delta) \\ \hline C_c(\delta) & D_c(\delta) \end{array}\right] = \left[\begin{array}{cc|c} A_\delta^c(\delta) & 0 & B_\delta^c(\delta) \\ B_o^c C_\delta^c(\delta) & A_o^c & B_o^c D_\delta^c(\delta) \\ \hline 0 & C_o^c & 0 \end{array}\right]. \tag{11}$$

The closed-loop state-space system from disturbance input $f_d$ to measured output $v$ is then given by

$$\left[\begin{array}{c|c} \dot{x}_{cl} & \\ \hline v & \end{array}\right] = \left[\begin{array}{c|c} \mathcal{A}(\delta) & \mathcal{B}(\delta) \\ \hline \mathcal{C}(\delta) & \mathcal{D}(\delta) \end{array}\right] \left[\begin{array}{c|c} x_{cl} & \\ \hline f_d & \end{array}\right], \tag{12}$$

where $x_{cl}^T = [x^T\ x_c^T]^T$ and

$$\left[\begin{array}{c|c} \mathcal{A}(\delta) & \mathcal{B}(\delta) \\ \hline \mathcal{C}(\delta) & \mathcal{D}(\delta) \end{array}\right] = \left[\begin{array}{cc|c} A & -BC_c(\delta) & B \\ B_c(\delta)C & A_c(\delta) & 0 \\ \hline C & 0 & 0 \end{array}\right]. \tag{13}$$

Note that (12) is affine in the scheduling parameter $\delta$. Stability of affine parameter dependent systems such as (12) can be assessed by solving a set of LMIs. The complexity of this set depends on the allowed rate of variation of the scheduling parameter. In our application, the operating condition of the mounted machine may be changed arbitrarily

and hence the scheduling parameter may vary arbitrary fast. Affinely parameterized system (12) with an arbitrary fast varying parameter $\delta \in [\underline{\delta}, \overline{\delta}]$ is quadratically stable if and only if there exists $K = K^T \succ 0$ such that [8]

$$\mathcal{A}(\delta)^T K + K\mathcal{A}(\delta) \prec 0 \quad \text{for all } \delta \in \{\underline{\delta}, \overline{\delta}\}. \qquad (14)$$

Our application aims at reducing sinusoidal disturbances within the frequency range 4 to 10 Hz and therefore the scheduling parameter will be restricted to lie within the interval $\delta \in [2\pi 4, 2\pi 10]$. The LMI solver SeDuMi [9] is successfully used to find a positive definite matrix $K \in \mathbb{R}^{10\times 10}$, which satisfies (14). We now have that system (12) is stable for arbitrarily fast parameter variations in the range $\delta \in [2\pi 4, 2\pi 10]$.

## V. Interconnection of the Spectrum Analyzer and the Controller

Since both the real-time spectrum analyzer and the LPV controller (10) have been designed, they can be interconnected to obtain the complete control setup. Several measured signals could be used to identify the dominating disturbance frequency. A logical first choice would be to use the vertical velocity $v$ of the AVIS since the goal of the controller is to minimize this velocity. A better alternative is to use the controller output $u$ as the input to the spectrum analyzer, because in contrast to the vertical velocity of the AVIS, the amplitude of the disturbance frequency will not decrease due to the suppression of the controller in this signal. As long as the disturbance is acting on the AVIS, its frequency is present in the controller output. A schematic overview of the complete control system is shown in Figure 7.

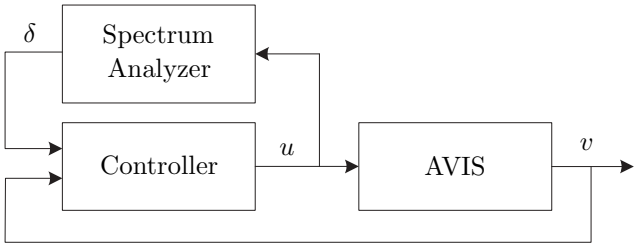


Fig. 7. Schematic representation of the implementation of the controller and the spectrum analyzer.

## VI. Simulation

To validate the proposed control setup, a simulation is performed. In this simulation the AVIS is subjected to a sinusoidal disturbance $f_d$ to simulate a disturbance force that acts on the payload. The amplitude of the sinusoid is constant, but the frequency of the disturbance force is continuously varying. The controller is implemented in three different ways. During the first 50 seconds, the original LTI controller (2) is applied. After 50 seconds the LPV controller (10) is used, where the scheduling parameter $\delta$ is taken to be the actually applied sinusoidal disturbance $f_d$. Finally, after 100 seconds, the controller implementation from Figure 7 is used and the scheduling parameter is replaced with the estimated frequency of the dominating disturbance. The disturbance isolation performance is depicted in Figure 8, where the spectrum of the vertical velocity $v$ is shown. It is obvious that the LPV controller achieves a much better disturbance rejection than the original controller. A slight increase of the vertical velocity is observed when the LPV controller is scheduled with the estimated frequency instead of the actually applied disturbance frequency, especially at low frequencies. This is caused by the delay that is introduced by the real-time spectrum analyzer. In the following section the proposed control setup is applied to the experimental setup.

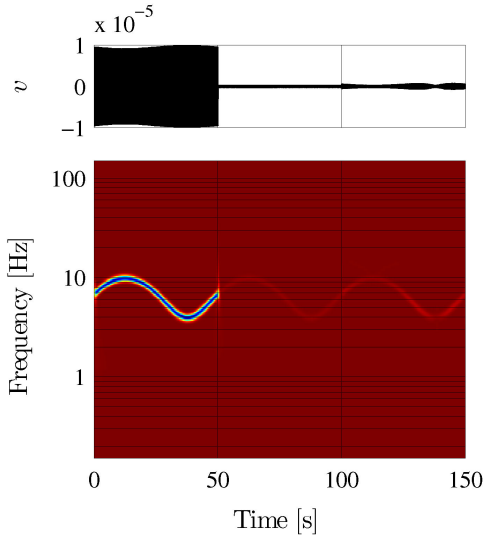


Fig. 8. Simulated signal $v$ and its spectrum. Dark red indicates no frequency content while blue indicates maximum frequency content.

## VII. Experimental Results

In this section, experiments will be performed on the experimental setup as depicted in Figure 3. The rotating imbalance is used to generate disturbance forces $f_d$ that directly act on the payload. The imbalance is represented by a mass $m_d$ located at a distance $e_d$ from the center of rotation. For constant angular velocities $\omega_d$, the induced disturbance force on the payload equals

$$f_d = m_d e_d \omega_d^2 \sin(\omega_d t). \qquad (15)$$

These disturbance forces are sinusoids with frequency $\omega_d/2\pi$ Hz and an amplitude that is proportional to $\omega_d^2$. The rotational velocity of the mass can vary in time, but is restricted between 4 and 10 revolutions per second. As mentioned before, environmental disturbances are present as well, but disturbances from the rotating mass dominate the disturbance spectrum.

During this experiment, the rotational velocity $\omega_d$ of the imbalance is controlled to vary continuously between 4 and 10 revolutions per second. The variation is obtained by using a sinusoidal reference velocity profile for the imbalance with a frequency of 0.02 Hz. The first half of the experiment, up to 50 seconds, the original LTI controller (2) is applied to be

able to quantify the performance improvement of the LPV controller. After 50 seconds the LPV controller (10) is used together with the real-time spectrum analyzer. Figure 9 shows the estimated frequency of the dominating disturbance by the real-time spectrum analyzer. The measured vertical velocity $v$ of the AVIS and the off-line computed time-frequency spectrum are depicted in Figure 10. Several observations can be made from this figure. The overall error is decreased by a factor 3 to 5, depending on the disturbance frequency. When the LPV controller is scheduled to increase the performance around 10 Hz an increase in the error level in the frequency range 10 to 15 Hz can be observed. This is in agreement with Figure 6, where it was shown that the application of a notch around 10 Hz results in amplification of the environmental disturbances in that range. As a final observation we note that there is a frequency component around 130 Hz in the vertical velocity of the payload. Although this cannot be explained from the first principles model of the isolator (1), frequency response measurements show that indeed a resonance frequency is present in this range. It is clear from this experiment that the LPV controller can offer a major increase in performance.

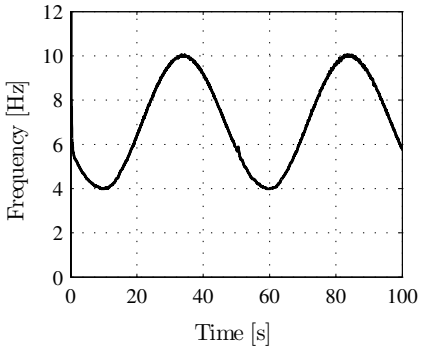


Fig. 9. Estimated frequency.

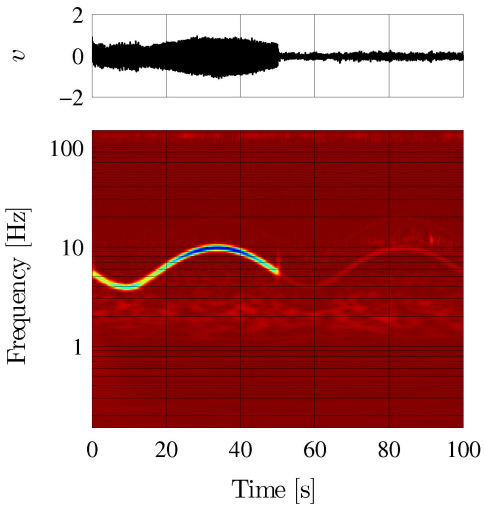


Fig. 10. Measured signal $v$ and its spectrum. Dark red indicates no frequency content while blue indicates maximum frequency content.

## VIII. Conclusions

In this paper we proposed a nonlinear controller setup for the active control of a vibration isolation system. This setup consists of two parts: (i) a real-time multiresolution spectrum analyzer that is able to identify the currently dominating disturbance, and (ii) an LPV controller that adapts itself to the available disturbance information. This resulted in a control system that is able to adapt itself to the current operating condition resulting in a closed-loop system with an overall increased performance when compared to an LTI controller.

The part of the controller that was scheduled according to the identified disturbance frequency was a notch filter. Such a notch filter has a certain width and reduction factor. These design parameters should be chosen with the application and expected disturbance variation in mind. A wide notch with a large reduction factor results in good disturbance reduction properties around the center frequency of the notch. However, at the same time environmental disturbances in other frequency regions will be amplified by such a notch. A too narrow notch with a small reduction factor on the other hand may not be adequate to reduce the dominating disturbance at the center frequency.

The proposed control system was validated by experiments that were performed on an active vibration isolation system. Compared to the originally designed LTI controller, the LPV control system was able to decrease the error by a factor 3 to 5 in case the disturbance spectrum is dominated by a single sinusoid with varying frequency.

## References


[1] C. Julian Chen, *Introduction to Scanning Tunneling Microscopy*. Oxford University Press, 2007.

[2] H. Yoshioka, Y. Takahashi, K. Katayama, T. Imazawa, and N. Murai, "An active microvibration isolation system for hi-tech manufacturing facilities," *Journal of Vibration and Acoustics*, vol. 123, no. 2, pp. 269–275, 2001.

[3] L. Zuo and J.-J. Slotine, "Active control vibration isolation using dynamic manifold," *The Journal of the Acoustical Society of America*, vol. 122, no. 6, p. 3148, 2007.

[4] E. Rivin, *Passive vibration isolation*. New York: ASME, 2003.

[5] P. Flandrin, *Time-Frequency/Time-scale analysis*. London, UK: Academic Press, 1999.

[6] M. Vrhel, C. Lee, and M. Unser, "Rapid computation of the continuous wavelet transform by oblique projections," *IEEE Trans. Signal Processing*, vol. 45, no. 4, pp. 891–900, 1997.

[7] M. Heertjes, N. van de Wouw, and W. Heemels, "Switching control in active vibration isolation," in *Proceedings of the 6th EUROMECH Nonlinear Oscillations Conference (ENOC)*, Saint Petersburg, Russia, 2008.

[8] C. Scherer, "Robust mixed control and LPV control with full block scalings," in *Advances in linear matrix inequality methods in control*, L. Ghaoui and S. Niculescu, Eds. Philadelphia: Siam, 1999.

[9] J. Sturm, "Using SeDuMi 1.02, a Matlab toolbox for optimization over symmetric cones," *Optimization methods and software*, vol. 11-12, pp. 625–653, 1999.